Korean Journal of Chemical Engineering
https://doi.org/10.1007/s11814-024-00265-4

ORIGINAL ARTICLE

Effects of Hydrothermal Carbonization Process Parameters on Physicochemical Properties and Combustion Behavior of Maize Stalk Hydrochars

Zhenghao Zhang[1,2] · Xin Shen[1] · Yingyi Zhang[1] · Zhichen Han[1] · Chunyin Zhang[1]

Received: 16 May 2024 / Revised: 7 July 2024 / Accepted: 14 August 2024

Abstract
Hydrothermal carbonization (HTC) is an effective method to improve the performance of biomass fuels. In this work, the reusable maize stalk (MS) hydrochars were prepared at different carbonization conditions, and the effects of carbonization parameters on physicochemical properties, recovery rate, coalification mechanism and combustion behavior of MS hydrochars were investigated. The results show that with the increase of temperature and time, the particle size, O/C and H/C ratios, flammability index and comprehensive combustion characteristic index of MS hydrochars decrease gradually, while the calorific value, ignition temperature (T_i), and burnout temperature (T_f) increase gradually. The combustibility and combustion reactivity of MS hydrochars are significantly better than anthracite. Under the optimal carbonization conditions (260 ℃, 40 min, solid–liquid ratio of 2%), MS hydrochar has a high carbon content and calorific value, and the carbon content and calorific value of MS are 66.85 and 22.36 MJ·kg^{-1}, respectively. HTC technology can effectively transform MS biomass into high energy density solid fuel, which provides a theoretical basis for expanding the application field of hydrochars.

Keywords Hydrothermal carbonization · Hydrochar · Physicochemical properties · Coalification mechanism · Combustion behavior

Introduction

Waste straw resource is a kind of renewable by-product produced in the process of agricultural production, which has the characteristics of wide distribution, huge yield and low price [1, 2]. China is a big agricultural country, with straw production reaching 977 million tons in 2022 alone. Therefore, straw resources have a wide range of application prospects and economic value. At present, the main treatment methods of straw resources are direct incineration, biomass fuel, biomass gasification, straw organic fertilizer, soil amendment, nutrients recovery, water remediation and so on [3–7]. In situ burning of straw resources not only causes serious environmental pollution, but also causes serious waste of resources and energy [8]. Under the dual pressure of energy and environmental issues, the use of straw biomass resources as renewable fuel has the advantage of zero carbon dioxide emissions, and received widespread attention around the world [9, 10]. China has huge corn stalk biomass resources, and China's maize stalk production reached 340 million tons in 2022 alone. In China, the comprehensive utilization rate of straw is only 65%, and the annual waste of maize stalk resources is about 119 million tons. Therefore, using maize stalk as biomass renewable energy has great economic and environmental benefits.

At present, hydrothermal carbonization (HTC) is considered as a promising biomass carbonization technology, which can convert organic matter in biomass resources into carbon products with high calorific value and energy density at a lower temperature [11, 12]. The hydrothermal carbon products have excellent grindability and reduce the cost of powder efficiency. Hydrothermal carbonization process has no requirement on the moisture content of the original biomass resources, and can directly deal with the biomass raw materials with high moisture content [11]. The dehydration and decarboxylation reactions in the hydrothermal

✉ Yingyi Zhang
zhangyingyi@ahut.edu.cn

[1] School of Metallurgical Engineering, Anhui University of Technology, Maanshan 243002, Anhui Province, China

[2] Shanghai Meishan Iron and Steel Limited by Share Ltd, Nanjing 210039, Jiangsu Province, China

Published online: 31 August 2024

carbonization process are exothermic reactions, which can release 1/3 of the heat required for hydrothermal carbonization, and the carbonization temperature and energy consumption are significantly lower than that of the pyrolytic carbonization process [13]. In addition, the hydrothermal carbonization process can remove a large number of water-soluble salts (potassium salt, sodium salt, chlorine salt, etc.) in biomass, and the content of ash and harmful elements in biomass hydrothermal charcoal greatly reduced [14–16]. Ma et al. [17] investigated the carbonization behavior of hydrothermal carbon from wheat straw and the physicochemical properties of wheat stalk biochar. Sobek et al. [18] investigated the combustion kinetics of biochar from hydrothermal carbonization of waste straw. Xu et al. [19] investigated the physical and chemical properties of rice husk hydrochar. The results show that the straw biochar has the characteristics of higher carbon content, lower ash content and less impurity elements, such as sulfur and phosphorus [20–22]. In addition, straw biochar also has the advantages of large porosity, pore volume and specific surface area, high heating value and excellent combustion performance [23]. Yuan et al. [24] investigated the possibility of replacing fossil fuels with biomass reducers in the rotary hearth furnace direct reduction process. Suopajärvi et al. [25] investigated the application of biomass fuel in blast furnace ironmaking and suggested that more systematic efforts should be made to achieve the transition from fossil reducing agents to biological reducing agents. With the increasing global crude steel production, metallurgical enterprises have a growing demand for fossil fuels, such as coke, coal, oil, and natural gas, which exacerbates the greenhouse effect, environmental pollution, and energy consumption [26–28]. Renewable biomass fuels have the characteristics of clean environmental protection and zero CO_2 emissions, and have received widespread attention from the metallurgical industry [29]. Suopajarvi et al. [25] discussed the possibility of renewable biomass carbon to replace some fossil energy in the process of ironmaking, and believed that biomass carbon replacing some parts of pulverized coal can effectively reduce the carbon emissions of blast furnace ironmaking. Wang et al. [30] reported that biomass hydrochar has the characteristic of being carbon neutral, blast furnace injection hydrochar can reduce CO_2 emissions, and every 1 kg/tHM of biomass hydrochar can reduce CO_2 emissions by 1.95 kg/tHM. Therefore, the straw biochar prepared by hydrothermal carbonization technology has the potential to replace pulverized coal as a metallurgical reducing agent and fuel [31, 32].

In this work, the maize stalk biomass resources are used to prepare renewable biochar through a hydrothermal carbonization process. The effects of hydrothermal carbonization parameters (carbonization temperature, carbonization time, and solid–liquid ratio) on physicochemical properties, recovery rate, chemical composition, and fuel ratio of MS hydrochars were investigated. Moreover, the combustion behavior and characteristics of MS hydrochars prepared at various hydrothermal carbonization parameters were also examined by a TG-DTG method.

Experimental Materials and Methods

Raw Materials

In this work, maize stalk (MS) was used as the raw material of hydrothermal carbonization, and 75% ethanol reagent was used to clean the quartz crucible of high-pressure reactor. Table 1 shows the proximate analysis, elemental analysis, and calorific value of the original maize stalk and anthracite. The fixed carbon (FC_{ad}) content, ash (A_{ad}) content, and calorific value of anthracite are much higher than that of maize stalk raw materials. It is worth noting that the volatile content of maize stalk is 76.45 wt%, which is much higher than the volatile (V_{ad}) content of anthracite (8.36 wt%). Therefore, maize stalk biomass resources cannot be directly used as metallurgical fuel and reducing agent. In order to meet the smelting requirements of metallurgical industry, the organic matter in maize stalk must be converted into carbon products with higher calorific value and energy density by hydrothermal carbonization process.

Preparation of Maize Stalk Hydrochars

The pretreatment process and parameters of maize stalk are shown in Fig. 1a. First, the MS raw materials were dried by an electric drying oven at 120 ℃ for 2 h, then the dried MS was crushed to the particle size below 5 mm. Second, the hydrothermal carbonization reaction of maize stalk was carried out through a mechanical stirring high-pressure reactor (TGYF-0.25, China), and the experimental equipment and process parameters for hydrothermal

Table 1 Proximate analysis and calorific value analysis of maize stalk and anthracite

Sample	Proximate analysis (wt%)				Elemental analysis (wt%)					Calorific value ($MJ \cdot kg^{-1}$)
	Fixed carbon	Volatiles	Ash	Moisture	C	H	O	N	S	
Maize stalk	16.34	76.45	3.07	3.23	46.28	6.13	43.36	0.72	0.21	16.25
Anthracite	78.25	8.36	12.27	1.12	79.85	2.98	2.27	1.13	0.68	24.31

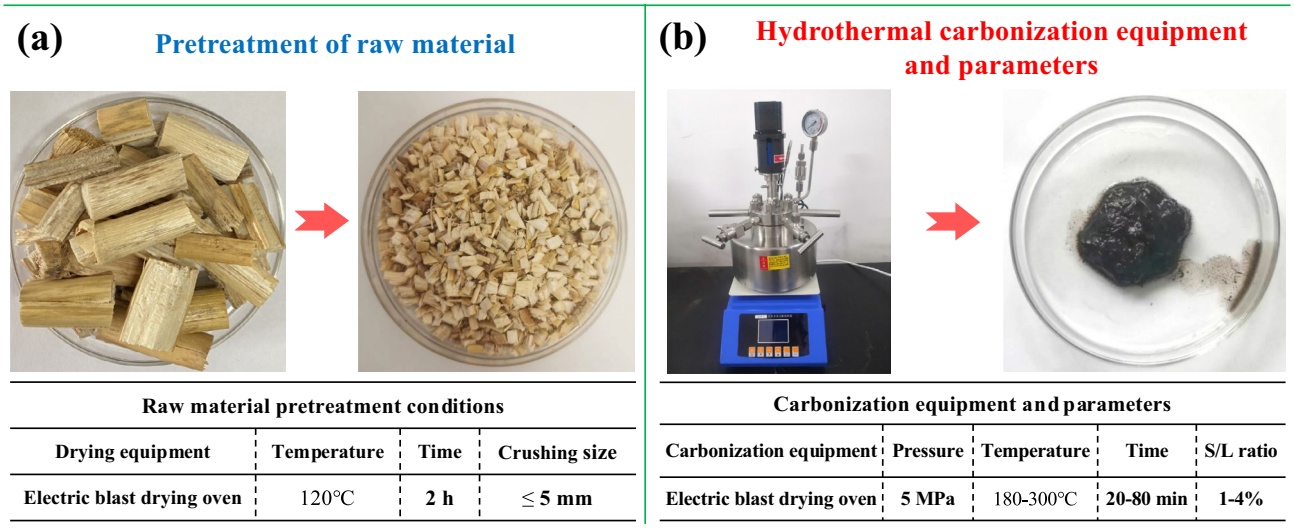

Raw material pretreatment conditions

Drying equipment	Temperature	Time	Crushing size
Electric blast drying oven	120°C	2 h	≤ 5 mm

Carbonization equipment and parameters

Carbonization equipment	Pressure	Temperature	Time	S/L ratio
Electric blast drying oven	5 MPa	180-300°C	20-80 min	1-4%

Fig. 1 Experimental equipment and parameters for pretreatment and hydrothermal carbonization of maize stalk. **a** Raw material pretreatment; **b** Hydrothermal carbonization equipment and parameters

carbonization are presented in Fig. 1b. The hydrothermal carbonization experiments were conducted at different carbonization temperatures (180, 220, 260, and 300 ºC), carbonization times (20, 40, 60, and 80 min), and solid–liquid ratios (1, 2, 3, and 4%) in a high-pressure reactor at a pressure of 5 MPa and a speed of 200 rpm. In this work, a single factor experimental scheme was used for the hydrothermal carbonization of corn stalks. The effect of different carbonization temperatures on the hydrothermal carbonization of maize stalk was investigated under fixed carbonization time (40 min) and solid–liquid ratio (3%) conditions. The effect of different carbonization times on the hydrothermal carbonization of maize stalk was investigated under fixed carbonization temperature (260 ºC) and solid–liquid ratio (3%) conditions. The effect of different solid–liquid ratios on the hydrothermal carbonization of maize stalk was investigated under fixed carbonization time (40 min) and temperature (260 ºC) conditions. After the hydrothermal carbonization, the high-pressure reactor was cooled to room temperature, the MS hydrochars solution in the quartz crucible was filtered with 40 mesh filter paper, and the filtered MS hydrochars was put into a drying oven to dry at 150 ºC for 3 h, respectively. Finally, the dried MS charcoal was weighed and crushed for subsequent experiments and analysis. The MS hydrochars prepared under different hydrothermal carbonization temperatures were named MS-HTC180, MS-HTC220, MS-HTC260, MS-HTC300, respectively. The MS hydrochars prepared under different hydrothermal carbonization times were named MS-HTC20, MS-HTC40, MS-HTC60, MS-HTC80, respectively. The MS hydrochars prepared under different hydrothermal carbonization times were named MS-HTC1, MS-HTC2, MS-HTC3, and MS-HTC4, respectively.

Physicochemical Properties Characterization

The Elemental Element Analyzer (VarioEL cube, Germany) was used for measuring the chemical element composition of MS and MS hydrochars. The industrial analysis of MS biomass resources was determined in accordance with the American Society for Materials and Testing (ASTM) standard E870-82 (2019), and the industrial analysis of anthracite (fixed carbon, ash, volatile matter and moisture) was determined in accordance with the national standard (GB/T212-2008). In addition, the X-ray diffractometer (Bruker D8ADVANCE, Germany) is used for phase composition analysis of MS hydrochars products prepared under different hydrothermal carbonization process parameters. The diffraction target of XRD test was Cu target (Cu-Kα, λ = 1.5406 A), the scanning Angle was 10 ~ 90°, and the scanning speed was 5°/min.

Combustion Properties Test

In order to investigate the influence of hydrothermal carbonization process on the combustion behavior of MS hydrochars, a synchronous thermal analyzer (STA 449 F3, Germany) was used to test the combustion of MS hydrothermal carbonization products. The Al_2O_3 crucible (85 μL) was used for the combustion experiment of MS hydrochars, the sample weight was about 6 mg, the experimental temperature was room temperature to 1000 ºC, the heating rate was 10 ºC·min^{-1}, the experimental atmosphere was air

atmosphere, and the gas flow was 100 mL·min^{-1}. The thermogravimetric curves (TG), derivative thermogravimetric analysis curves (DTG) and heat absorption or heat release rate curves (DSC) of MS hydrochars were obtained by thermal analysis experiments. The combustion conversion rate (α) is calculated using data recorded by a weight loss curve (TG-DTG). The calculation formula is as follows:

$$\alpha = \frac{m_0 - m_t}{m_0 - m_\infty}, \tag{1}$$

where m_0 is the initial mass of the sample (mg), m_t is the mass of the sample at the reaction time t (mg), m_∞ is the mass of the sample at the end of the reaction (mg).

In this work, TG-DTG method was used to determine the combustion characteristics of MS hydrochars prepared at various carbonization parameters. According to the TG-DTG curve, the initial combustion temperature (T_i), burnout temperature (T_f), maximum reaction weight loss rate (R_{max}) and maximum weight loss rate temperature (T_m), flammability index (C) and comprehensive combustion index (S) of MS hydrochars can be estimated. The calculation formulas of flammability index and comprehensive combustion characteristic index are shown in Eqs. (2) and (3), respectively.

$$C = \frac{R_{max}}{T_i^2}, \tag{2}$$

$$S = \frac{R_{max} R_{mean}}{T_i^2 T_f}, \tag{3}$$

where R^{max} is the maximum combustion rate (wt%·min^{-1}), and Rmean is the average combustion rate (wt%·min^{-1}). Figure 2 shows the schematic diagram of the T_i and T_f of MS hydrochars.

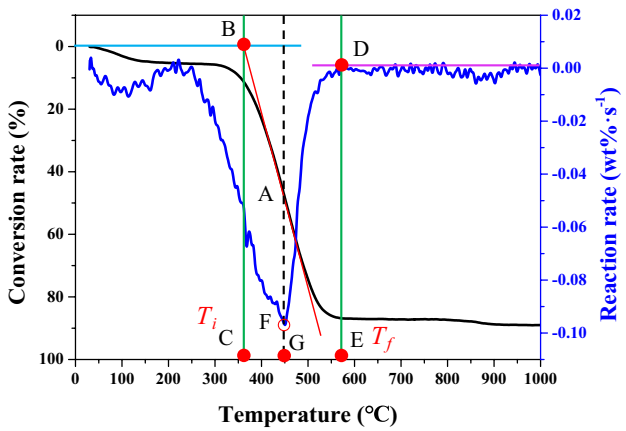

Fig. 2 Schematic diagram of T_i and T_f of MS hydrochars

Results and Discussion

Physicochemical Properties of Maize Stalk Hydrochars

Macroscopic Morphology and Recovery Rate

Figure 3 presents the influence of the hydrothermal carbonization parameters on the macroscopic morphology of MS hydrochars. The effect of hydrothermal carbonization temperature on the macroscopic morphology of MS hydrochars is shown in Fig. 3a–d. It can be seen that the higher the carbonization temperature, the better the carbonization effect. As show in Fig. 3a, the carbonization effect of MS is very poor under the carbonization temperature is 180 ℃, and the MS hydrochars almost maintain their original morphology. When the carbonization temperature is 220 ℃, the color of the MS hydrochars slightly darkens, and obvious fragmentation and agglomeration phenomena can be observed, as presented in Fig. 3b. It can be seen from Fig. 3c that the carbonization of MS is very obvious under the carbonization temperature is 260 ℃, and most of the MS have been completely carbonized into black brown powder. As shown in Fig. 3d, the carbonized products have been transformed into black powder under the carbonization temperature is 300 ℃, and the macro-morphology is very close to that of coal powder. Figure 3e–h presents the influence of the carbonization time on the macroscopic morphology of the MS carbonization products. As shown in Fig. 3e, the MS hydrochar is black block under the carbonization time is 20 min. When the carbonization time is 40 min and 60 min, the color and macroscopic morphology of the MS hydrochars products are very similar, both appearing as black brown powder. When the carbonization time is 80 min, the MS hydrochar product has been completely carbonized into black powder, which has a macro-morphology similar to that of pulverized coal. Figure 3i–l shows the influence of the solid–liquid ratio on the macroscopic morphology of the MS hydrochars products. The effect of solid–liquid ratio on the macroscopic morphology of MS biochars products is not obvious under the carbonization temperature is 260 ℃, and the MS biochars prepared with different solid–liquid ratios are black powder. In addition, it can be clearly observed that the higher the solid–liquid ratio, the higher the recovery rate of MS hydrochars. Although increasing the solid–liquid ratio can significantly improve the recovery rate of MS hydrochars, the density of maize stalk is very small, which greatly limits the further increase of the solid–liquid ratio.

After the hydrothermal carbonization, the dried MS hydrochar was weighed by an electronic balance, and then the recovery rate of MS hydrochars was calculated

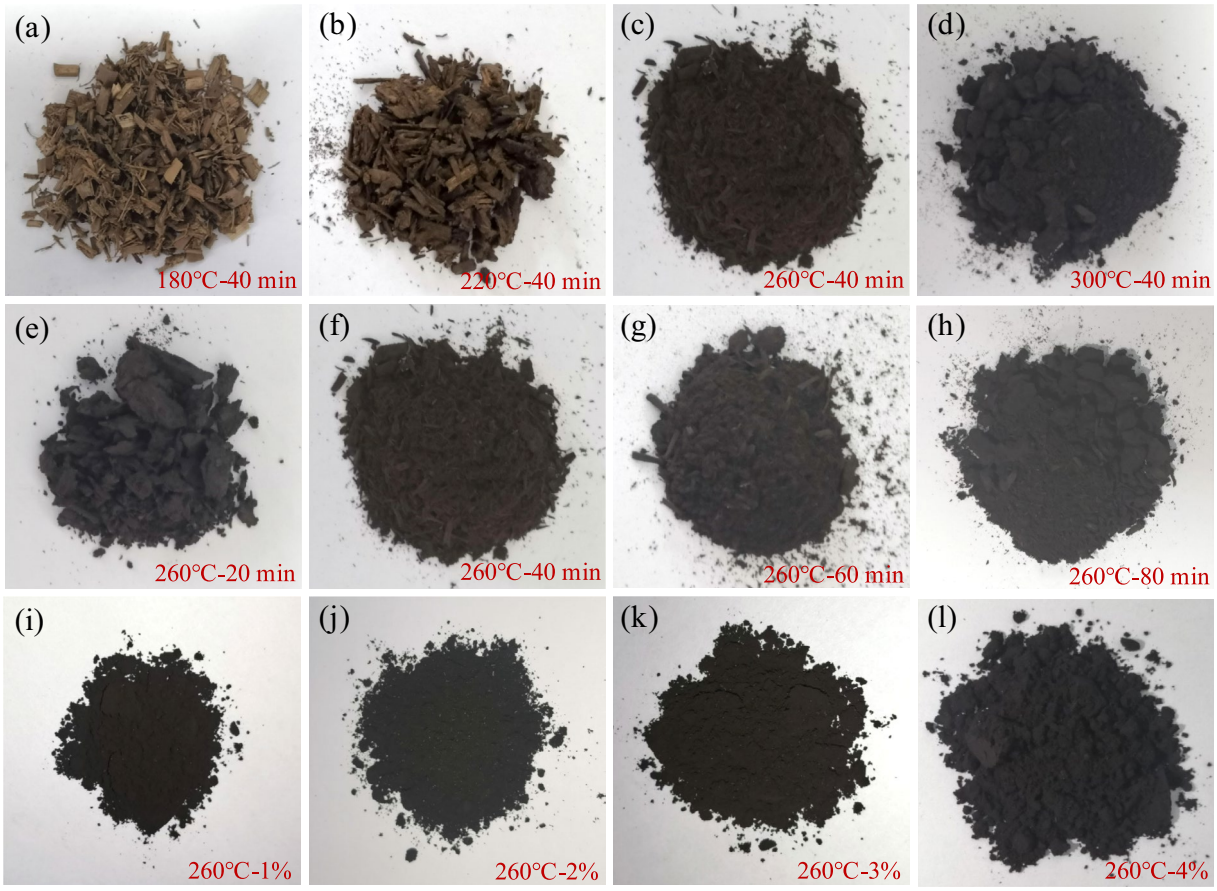

Fig. 3 Macroscopic morphology of MS hydrochars prepared at different hydrothermal carbonization parameters. **a–d** Carbonization temperature; **e–h** carbonization time; **i–l** solid–liquid ratio

according to the mass change before and after carbonization. Figure 4 shows the effect of hydrothermal carbonization parameters on the recovery rate of MS hydrochars. When the solid–liquid ratio is 2%, the higher the hydrothermal carbonization temperature and the longer the carbonization time, the lower the recovery rate of MS carbonization products, as shown in Fig. 4a and b. When the carbonization temperature is 180 ºC and 220 ºC, the recovery rates of MS hydrochars are 49.67% and 32.5%, respectively. This indicates that when the carbonization temperature is low, the dehydration, decarboxylation reaction, and lignin decomposition rate of MS are lower, and the hydrothermal carbonization effect of MS is poor. When the carbonization temperature is 260 ºC and 300 ºC, the recovery rates of the MS hydrochars are 20.29% and 14.88%, respectively. This indicates that increasing the carbonization temperature and time can improve the dehydration and decarboxylation reactions of MS, and promote the decomposition of lignin. Similarly, when the carbonization time is 20 min, the carbonization degree of MS is lower, and the recovery rate of MS hydrochars is the highest (33.08%). When the carbonization time increases to 40, 60, and 80 min, the recovery rate of MS hydrochars significantly decreases, and the recovery rates of MS hydrochars are 20.04%, 16.25%, and 13.88%, respectively. In addition, the solid–liquid ratio (mass ratio) has an obvious influence on the recovery rate of MS hydrochars. The higher the solid–liquid ratio, the greater the recovery rate of MS hydrochars, as listed in Fig. 4c. It can be seen that the recovery rate of MS hydrochars is only 18–22.5% under the solid–liquid ratio is 1–2%. When the solid–liquid ratio increases to 3% and 4%, the recovery rates of MS hydrochars are 32% and 41.53%, respectively.

Microstructure and Element Composition

The SEM images of the MS hydrochars prepared at different carbonization parameters are shown in Fig. 5, and the EDS results of the micro-zones are shown in Table 2. It can be seen that with the increase of hydrothermal carbonization temperature, carbonization time and solid–liquid ratio, the micro-morphology of maize stalk carbonization products has a significant change, and the larger the carbonization temperature and time, the smaller the particle size of carbonized

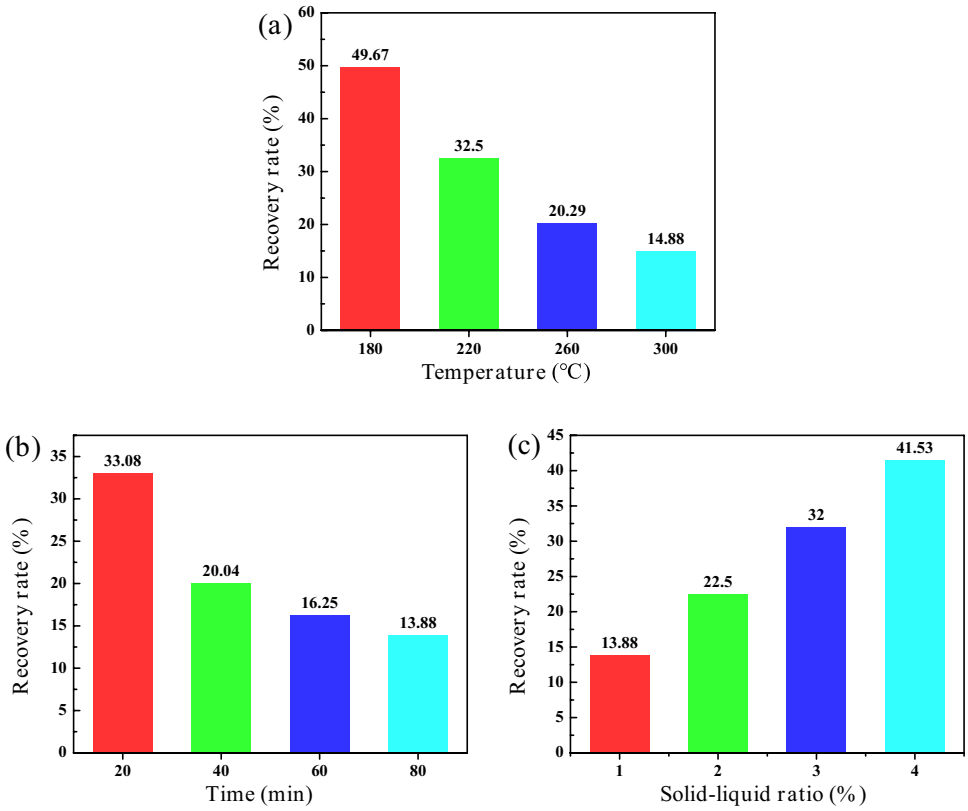

Fig. 4 The influence of hydrothermal carbonization parameters on the recovery rate of MS hydrochars. **a** Carbonization temperature; **b** carbonization time; **c** solid–liquid ratio

products. On the contrary, with the increase of solid–liquid ratio, the particle size of carbonized products increased significantly. Although high solid–liquid ratio can significantly improve the yield of carbonized products, it is not conducive to the hydrothermal carbonization reaction of maize stalk. As shown in Fig. 5a, the carbonized products still maintain larger particles under the carbonization temperature is between 180 and 220 ºC, and the content of C element is only 50.90–56.88 wt%. When the carbonization temperature increases to 260–300 ºC, the maize stalks have been decomposed into long strips and fine particles (< 50 μm), with a C element content of 71.96–74.36 wt% and an O element content of only 25.64–28.04 wt%. This indicates that a higher hydrothermal carbonization temperature is conducive to the carbonization of corn stalks. Figure 5b shows the effect of carbonization time on the microstructure of MS hydrochars. It can be seen that when the carbonization time is 20 min, the carbonization product particles are larger (> 4 mm), and the carbonization is not uniform, with a C content of only 60.57 wt%. When the carbonization time increases to 40–80 min, the large particle MS hydrochars has been completely decomposed into long and fine particle shapes (< 50 μm), with a significant increase in C element content (71.87–77.69 wt%) and a significant decrease in O element content (22.31–28.13 wt%). Therefore, when the carbonization time is 40–80 min, the MS hydrochars have good reactivity and high carbon content. Figure 5c shows the effect of the solid–liquid ratio on the microstructure of MS hydrochars. It can be seen that when the solid–liquid ratio is 1% and 2%, the maize stalk has been carbonized into fine strips and particles (< 50 μm), and this fine porous microstructure greatly improves the reactivity of the MS hydrochars, and the MS hydrochars have a high carbon content (75.34–78.21 wt%). When the ratio of solid to liquid is 3%, the size of MS hydrochars increases obviously, the content of C element decreases slightly. When the ratio of solid to liquid is 4%, the size of carbonized products reaches the millimeter level (> 2 mm), and the content of C element significantly decreases, and the content of C is only 55.68 wt%. Therefore, the MS hydrochars with higher carbon content and smaller particle size can be obtained when the carbonization temperature, time, and solid–liquid ratio are 260 ºC, 40 min, and 2%, respectively.

Chemical Composition and Fuel Ratio

The chemical composition of MS hydrochars obtained under different hydrothermal carbonization parameters is listed in Table 3. It can be seen that with the increase of hydrothermal carbonization temperature and time, the C content of MS hydrochars increases obviously, while the O content decreases significantly. In addition, increasing carbonization temperature and solid–liquid ratio can significantly increase S content in MS hydrochars, while increasing

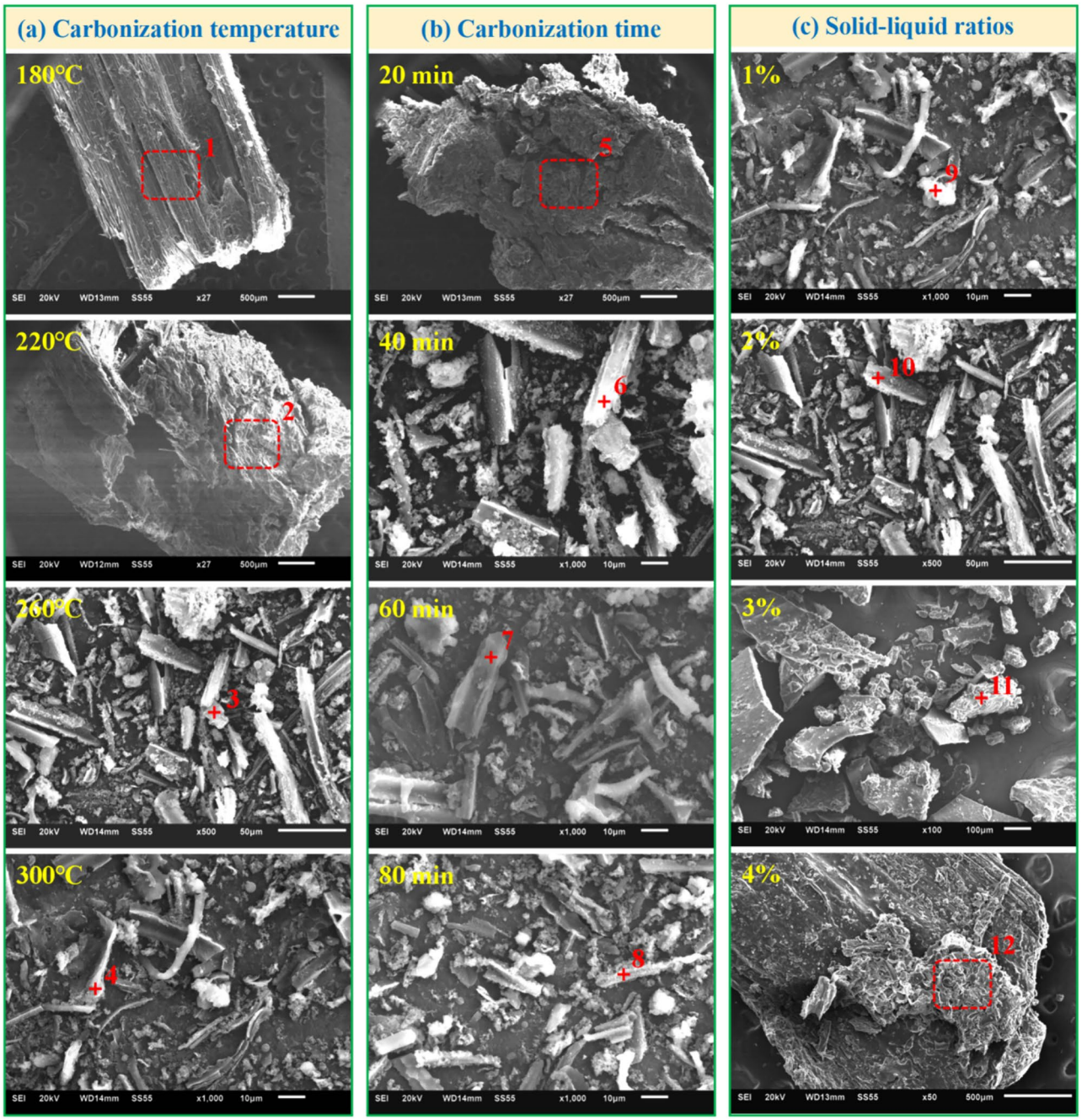

Fig. 5 SEM images of the MS hydrochars prepared at different carbonization parameters

Table 2 The EDS results of MS hydrochars prepared at different carbonization parameters

Element	Spot 1	Spot 2	Spot 3	Spot 4	Spot 5	Spot 6	Spot 7	Spot 8	Spot 9	Spot 10	Spot 11	Spot 12
C	50.90	56.88	71.25	74.36	60.57	71.87	72.35	77.69	78.21	75.34	73.49	55.68
O	49.10	43.12	28.75	25.64	39.43	28.13	27.65	22.31	21.79	24.66	26.51	24.32

Table 3 Chemical composition of MS hydrochars obtained under different hydrothermal carbonization parameters

Samples	Elemental analysis (wt%)					H/C	O/C	Calorific value ($MJ·kg^{-1}$)
	C	H	O	N	S			
MS	46.28	6.13	43.36	0.72	0.210	0.703	1.589	16.25
MS-HTC180	48.12	7.673	35.306	0.59	0.311	0.159	0.734	18.76
MS-HTC220	50.35	7.545	32.809	0.62	0.676	0.150	0.652	19.52
MS-HTC260	66.85	6.243	16.679	1.52	0.708	0.093	0.249	22.36
MS-HTC300	69.13	4.631	15.701	1.68	0.858	0.067	0.227	23.58
MS-HTC20	52.57	6.438	30.297	1.32	1.375	0.122	0.576	20.35
MS-HTC40	66.84	6.258	16.720	1.59	0.592	0.094	0.250	22.33
MS-HTC60	68.90	6.165	14.90	1.67	0.365	0.089	0.216	23.29
MS-HTC80	69.05	5.890	13.58	1.71	0.283	0.083	0.196	23.46
MS-HTC1	67.15	6.012	16.814	1.65	0.374	0.090	0.236	22.45
MS-HTC2	66.87	6.226	16.639	1.58	0.685	0.093	0.249	22.34
MS-HTC3	66.08	6.285	17.113	1.57	0.852	0.095	0.259	22.17
MS-HTC4	66.02	5.915	17.412	1.54	1.013	0.096	0.262	22.03
Anthracite	79.91	2.95	2.24	1.12	0.64	0.021	0.443	24.31

carbonization time can significantly reduce S content in MS hydrochars. The S content of MS hydrochars is 0.592 wt% under the carbonization time is 40 min, which is close to the S content in anthracite. When the carbonization time increases to 60–80 min, the S content in MS hydrochars is only 0.283–0.365 wt%, which is much lower than the S content in anthracite. Increasing the carbonization time is beneficial for reducing SO_2 emissions in the metallurgical industry, but excessive carbonization time will increase the production cost of MS hydrochars. In addition, increasing the hydrothermal carbonization temperature can significantly increase the calorific value of MS hydrochars, while carbonization time and solid–liquid ratio have little influence on the calorific value of MS hydrochars. The maximum calorific value (23.58 $MJ·kg^{-1}$) of MS hydrochars is obtained at carbonization temperature, time and solid–liquid ratio of 300 ºC, 40 min, 2%, respectively. It can be seen that the calorific value of MS hydrochar prepared at optimal process conditions is slightly lower than that of anthracite (24.31 $MJ·kg^{-1}$), which can meet the requirements of hydrochar fuel for blast furnace ironmaking.

The influences of hydrothermal carbonization temperature, time, and solid–liquid ratio on the volatile matter, fixed carbon, and fuel ratio (FC_{ad}/V_{ad}) of MS hydrochars are presented in Fig. 6. As shown in Fig. 6(a), the FC_{ad} content of the MS hydrochars is very low (25.93–30.25 wt%) under the carbonization temperature is 180 ºC and 220 ºC, while the volatile content is very high (58.92–65.28 wt%). However, when the carbonization temperature increases to 260–300 ºC, the FC_{ad} content of MS hydrochars significantly increases, while the V_{ad} content significantly decreases. The FC_{ad} content of the MS hydrochars is 62.9–66.97 wt%, the V_{ad} content only is 16.26–19.62 wt%. As presented in Fig. 6b, increasing the carbonization time can obviously increase the FC_{ad} content of MS hydrochars and reduce its volatile content. When the carbonization time is 20 min, the FC_{ad} and V_{ad} content of the MS hydrochars are 51.22 wt% and 33.70 wt%, respectively. At a carbonization time of 40 min, the FC_{ad} content of the MS hydrochars significantly increases, while the V_{ad} content significantly decreases. The A_{ad} content of the MS hydrochars is 12.82 wt%, and the FC_{ad} and V_{ad} content are 62.85 wt% and 19.54 wt%, respectively. It is worth noting that when the carbonization time is 60–80 min, the FC_{ad} content of the MS hydrochars slightly increases (66.95–67.14 wt%), while the volatile content slightly decreases (15.95–16.22 wt%), and the ash content remains almost unchanged (12.30–12.46 wt%). As presented in Fig. 6c, the effect of solid–liquid ratio on the fixed carbon and V_{ad} content of MS hydrochars is relatively small, and the FC_{ad} and V_{ad} content of MS hydrochars follow a linear variation pattern with the solid–liquid ratio. It can be seen that the higher the solid–liquid ratio, the lower the FC_{ad} content, and the higher the V_{ad} content, while the A_{ad} content is almost unaffected by the solid–liquid ratio. When the carbonization temperature is 260 ºC, the carbonization time is 40 min, and the solid–liquid ratio is 1%, the carbonization product has the maximum FC_{ad} content (65.02 wt%) and the lowest V_{ad} content (17.55 wt%). When the solid–liquid ratio is 2%, the FC_{ad} and V_{ad} content of MS hydrochars are 62.89% and 19.46%, respectively. When the solid–liquid ratio increases to 3–4%, the FC_{ad} content and V_{ad} content of MS hydrochars decreases slightly, and the lowest FC_{ad} content is 57.79 wt%.

The fuel ratio (fixed carbon/volatile matter) is an important indicator of the coalification degree, and the higher the fuel ratio, the higher the coalification degree. Figure 7 shows the influence of hydrothermal carbonization temperature, time and solid–liquid ratio on the fuel ratio of MS hydrochars. It can be seen that the increase of hydrothermal

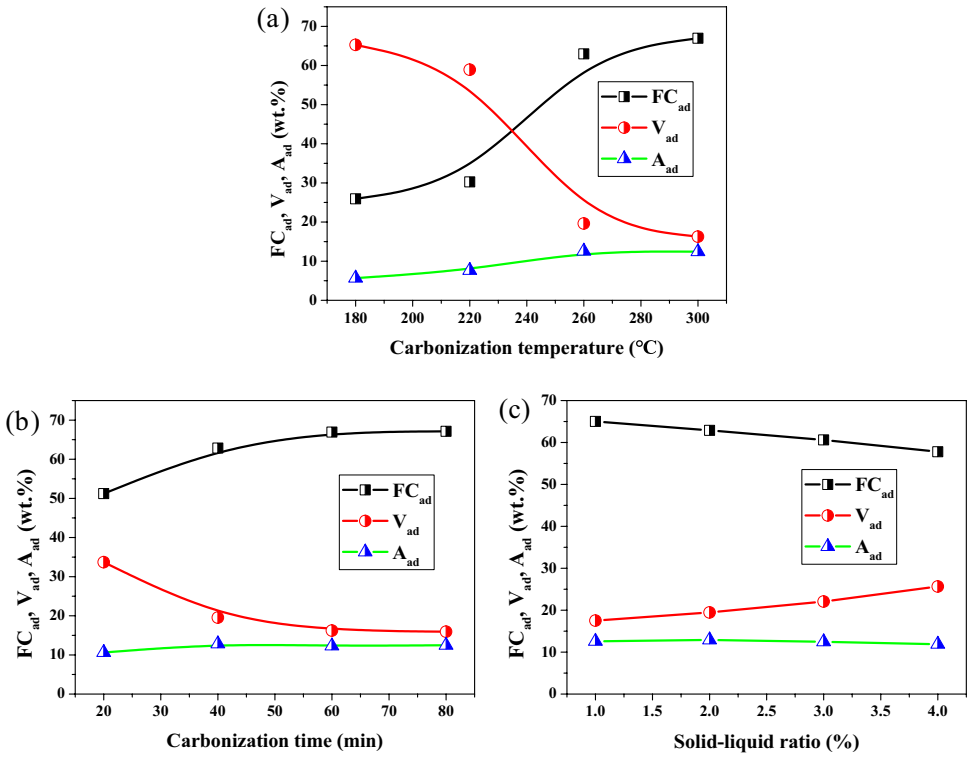

Fig. 6 The relationship curves between FC_{ad}, V_{ad} and A_{ad} content of MS hydrochars and hydrothermal carbonization parameters

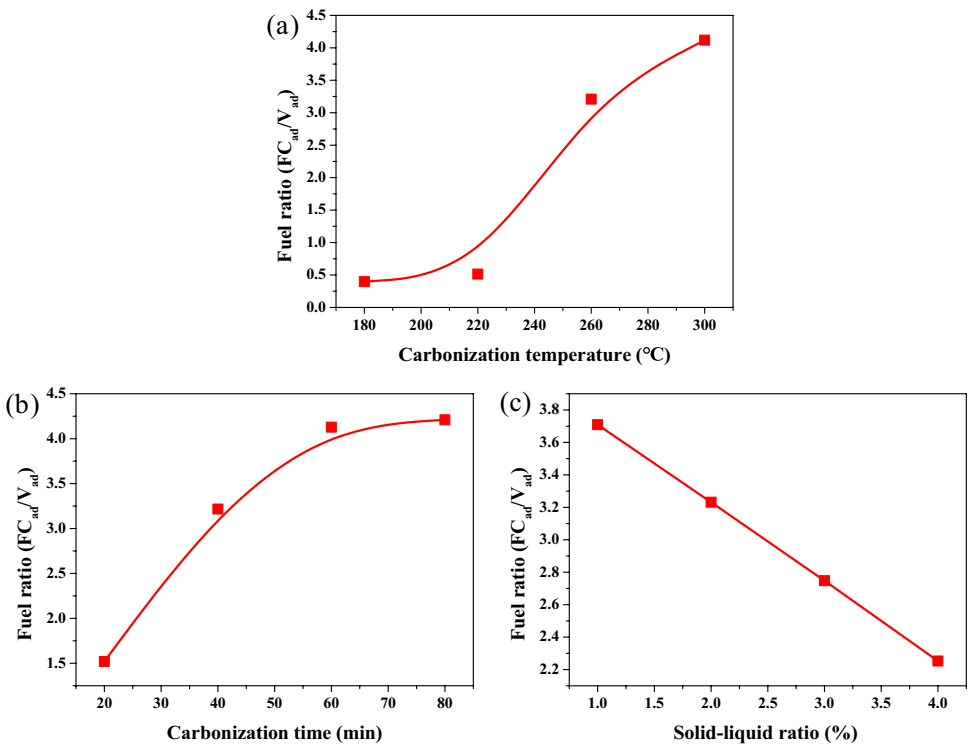

Fig. 7 Effect of hydrothermal carbonization process parameters on MS hydrochars fuel ratio

carbonization temperature and time can significantly increase the fuel ratio of hydrothermal carbon of corn stalk, but the increase of solid–liquid ratio will decrease the fuel ratio of MS hydrochars. When the carbonization time is 60 min and 80 min, the fuel ratio of MS hydrochars is similar, which indicates that excessive carbonization time has limited effect on improving the degree of coalification of MS hydrochars. When the carbonization temperature is 260 °C,

the carbonization time is 40 min, and the solid–liquid ratio is 2%, the fuel ratio of MS hydrochars is about 3.25, indicating that the MS hydrochars prepared under this process condition has a high degree of coalification.

Coalification Mechanism

The Van Krevelen diagram was proposed by Van Krevelen in 1961 to depict the coalification process of coal and its organic matter. Figure 8 presents the effect of hydrothermal carbonization parameters on the Van Krevelen map of organic matter in MS. According to the linear fitting results of H/C and O/C atomic ratios, there is a strong linear correlation between H/C and O/C in MS hydrochars ($R^2 = 0.934$–0.996). The linear fitting slopes for different carbonization temperatures, carbonization times, and solid–liquid ratios are 5.828, 10.266, and 4.429, respectively. This indicates that the influence of hydrothermal carbonization process parameters on H/C is much greater than on O/C, and the removal rate of H element is greater than that of O element. As shown in Fig. 8a and b, the Van Cleveland map can be divided into two regions under different carbonization temperatures and times. It can be observed that the H/C and O/C molar ratio of the MS hydrochars decreases significantly with the increase of hydrothermal carbonization temperature and time, which indicates that increasing the carbonization temperature and time can significantly improve the dehydrogenation and deoxygenation capacity during the hydrothermal carbonization process, and improve the carbonization degree and aromatization degree of MS. However, when the carbonization temperature and time are low, the H/C and O/C molar ratios of MS hydrochars are very large, indicating that there is still a large amount of original organic residue in MS hydrochars. Figure 8c shows the influence of solid-to-liquid ratio on the Van Krevelen map of MS hydrochars. It can be seen that the Van Cleef Villeneuve plots under different solid–liquid ratios can be divided into three regions. As the solid–liquid ratio increases, the H/C and O/C molar ratios of MS hydrochars slightly increase, which indicates that excessively high solid–liquid ratios are not conducive to the coalification of MS. The H and O content in hydrochars is related to the active sites, and the decrease in H/C and O/C ratio is mainly attributed to the dehydrogenation and dehydroxylation reactions during hydrothermal carbonization, as well as the decomposition of volatile organic compounds. Increasing the carbonization temperature and time can effectively promote the dehydrogenation, dehydroxylation reactions, and organic matter decomposition during the hydrothermal carbonization process of MS, while increasing the solid–liquid ratio can to some extent inhibit the carbonization rate of MS.

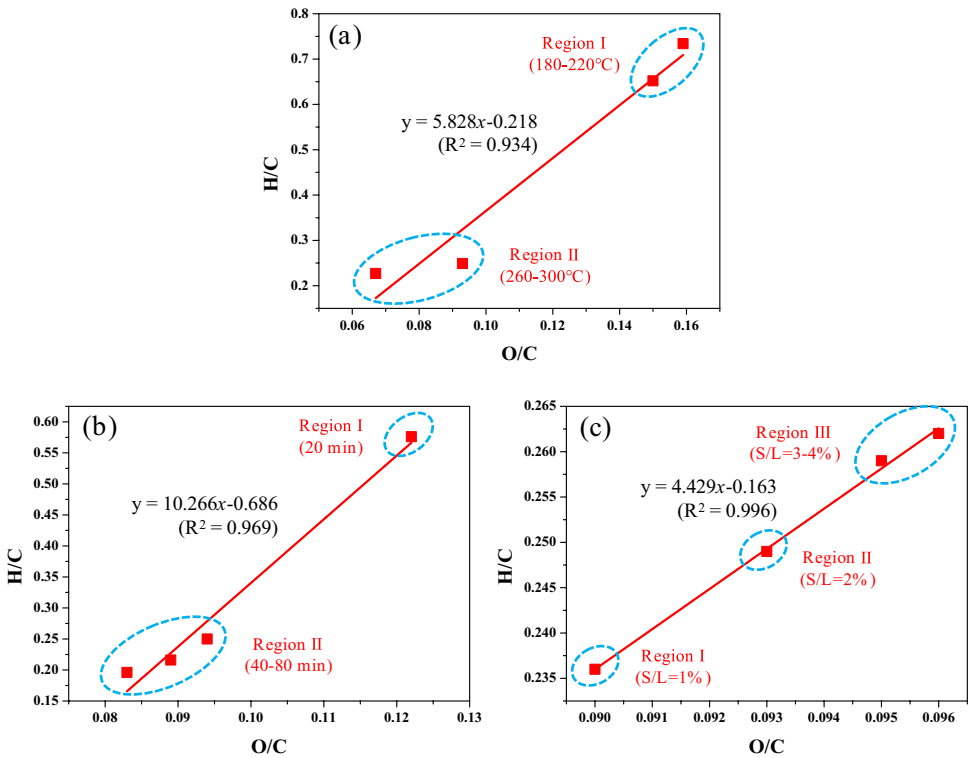

Fig. 8 Effect of hydrothermal carbonization parameters on the Van Krevelen map of organic matter in MS. **a** Carbonization temperature; **b** Carbonization time; **c** Solid-to-liquid ratio

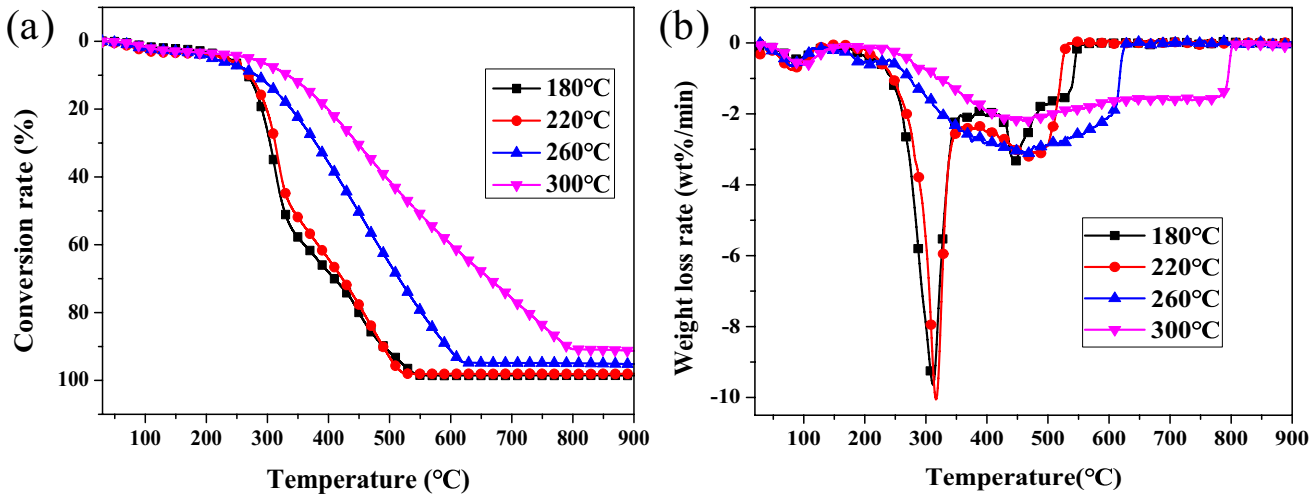

Fig. 9 Combustion conversion rate (**a**) and reaction rate (**b**) curves of MS hydrochars prepared at different carbonization temperatures

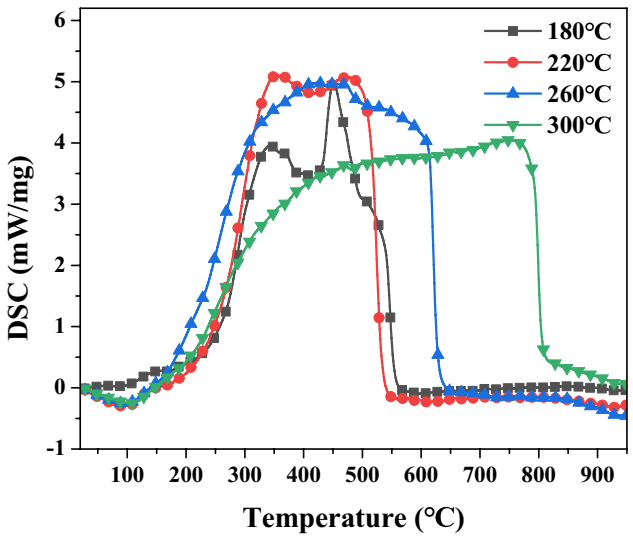

Fig. 10 DSC curves of MS hydrochars prepared at different carbonization temperatures

Combustion Behavior of Maize Stalk Hydrochars

Effect of Carbonization Temperature on the Combustion Behavior

The TG and DTG curves of MS hydrochars prepared at different carbonization temperatures are presented in Fig. 9, and the corresponding DSC curve is shown in Fig. 10. As shown in Fig. 9, there is no significant weight loss phenomenon before 200 ℃, and the main combustion stage of MS hydrochars is from 200 to 800 ℃. The combustion conversion rate and combustion rate significantly increased from 200 to 800 ℃, and the DSC curve also sharply increased, indicating that the MS hydrochars suffered severe combustion weight loss and heat release in this temperature range. The combustion process of MS hydrochars prepared at low carbonization temperature (180–220 ℃) is more complicated, and two obvious weight loss peaks are observed on TG and DTG curves, and two obvious exothermic peaks are also observed on DSC curves. The TG-DTG curves of MS hydrochars gradually move to the high temperature region with the increase of hydrothermal carbonization temperature. When the carbonization temperature is between 180 and 220 ℃, the TG-DTG curves of the carbonization products are located in the low temperature range, which is significantly lower than the known combustion temperature range of coal powder (500–700 ℃). It is noteworthy that when the carbonization temperature is between 260 and 300 ℃, the sharp DTG curve disappears, which may be related to the decomposition of cellulose [33, 34]. In addition, the width of the weight loss peak and the exothermic peak is very wide under the carbonization temperature is 260–300 ℃, indicating that the MS biochar prepared within this temperature range has a larger combustion temperature range.

According to the TG-DSC test data of MS biochar, the combustion characteristic parameters of MS hydrochars prepared at various carbonization temperatures are calculated, as presented in Fig. 11. It can be observed that with the increase of hydrothermal carbonization temperature, the T_i, T_f, and T_m of MS hydrochars all present a gradual increase trend, while the C and S show the opposite trend. This indicates that with the increase of hydrothermal carbonization temperature, the carbonization degree of MS hydrochars gradually increases, the combustion reactivity gradually weakens, and the MS hydrochars gradually evolve from more complex organic matter to biomass charcoal fuel

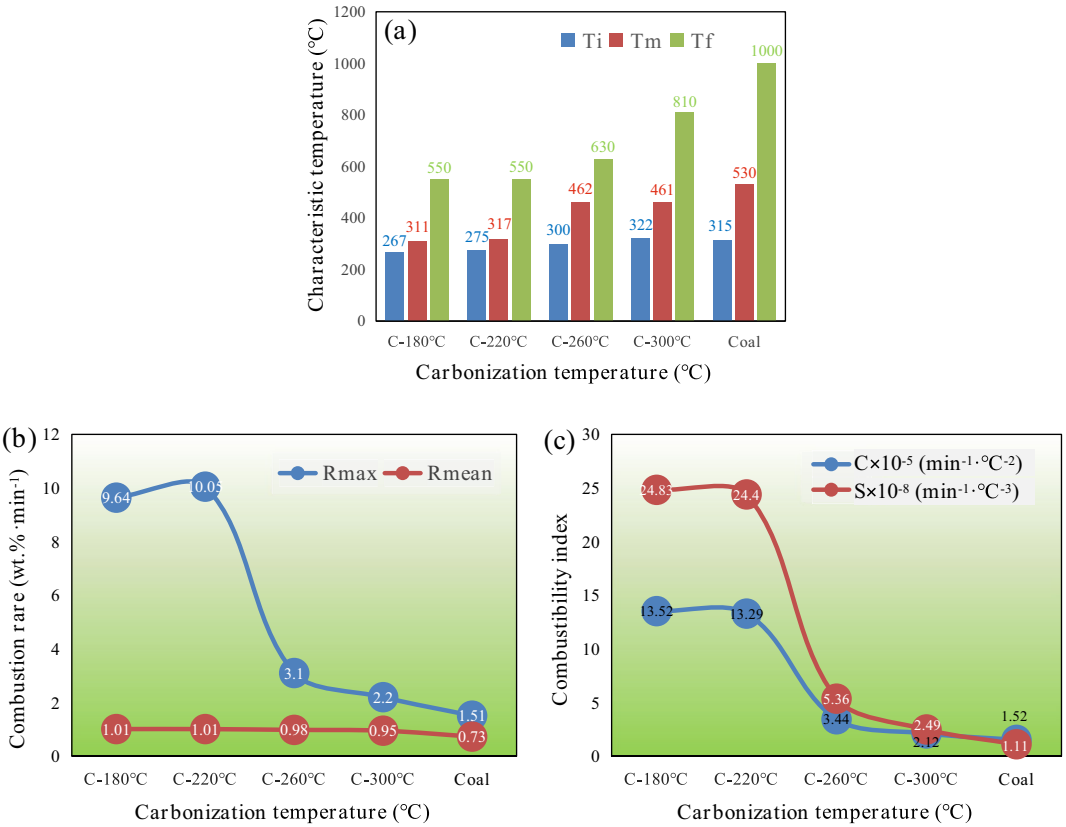

Fig. 11 The effect of carbonization temperature on the combustion characteristic parameters of MS hydrochars. **a** Characteristic temperature; **b** Combustion rate; **c** Combustibility index

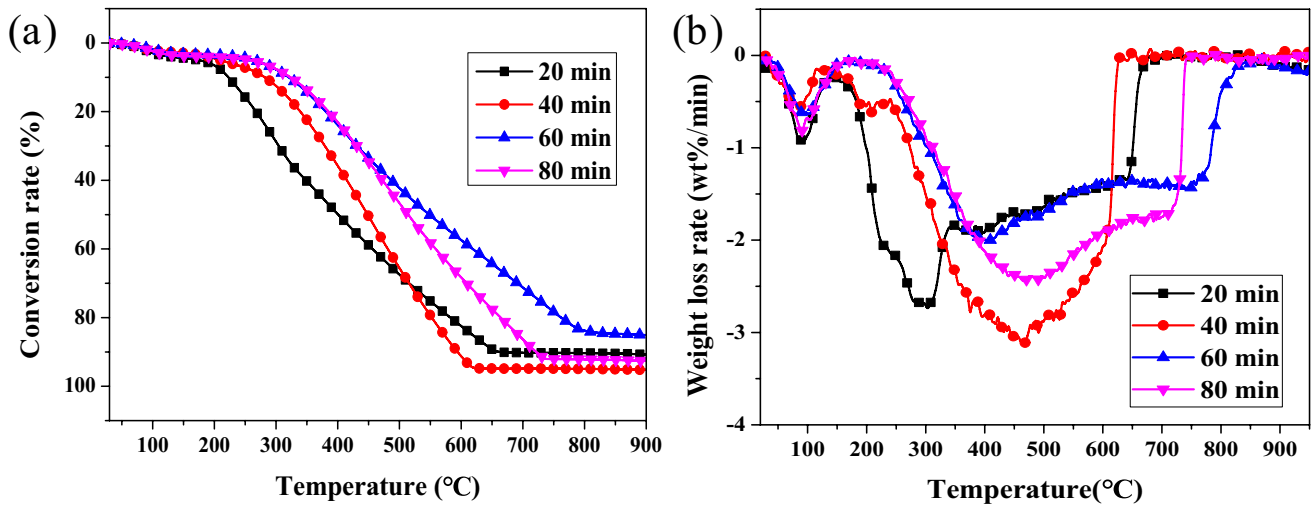

Fig. 12 Combustion conversion rate (**a**) and reaction rate (**b**) curves of MS hydrochars prepared at different carbonization times

similar to coal powder. In addition, the T_i and T_m of MS hydrochars are significantly lower than coal powder, while the *C* and *S* are significantly higher than coal powder, indicating that the combustibility and combustion reactivity of MS hydrochars are significantly better than coal powder.

Effect of Carbonization Time on the Combustion Behavior

The TG, DTG and DSC curves of MS hydrochars prepared at different carbonization times are presented in Figs. 12 and 13, respectively. It can be observed that no significant

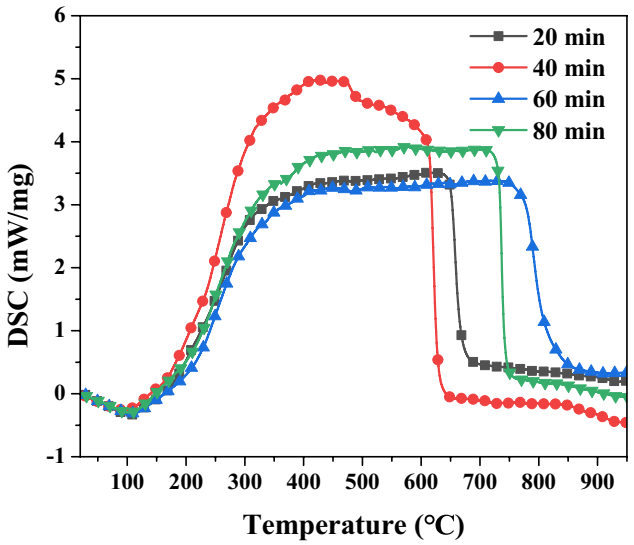

Fig. 13 DSC curves of MS hydrochars prepared at different carbonization times

combustion loss is observed before 200 ℃ for MS hydrochars, and the combustion of MS hydrochars is mainly concentrated at 200 ~ 800 ℃, and the MS hydrochars show a long combustion time and stable combustion characteristics. When the carbonization time is 40 min, the maximum combustion rate, the highest exothermic peak and the narrow combustion temperature range can be observed, and the carbonized products show better combustion performance. When the carbonization time is from 60 to 80 min, the corresponding weight loss curve and the exothermic peak are significantly wider, and the burning time is also extended, which indicates that the carbonization degree of MS hydrochars is significantly increased.

Based on the test data of TG-DSC of MS hydrochars, the combustion characteristic parameters of carbonization products under different hydrothermal carbonization times are calculated, as presented in Fig. 14. Figure 14a shows that with the increase of the carbonization time, the T_i, T_f, and T_m of MS hydrochars increase significantly. As presented in Fig. 14b, the carbonization time has little effect on the maximum combustion rate (R_{max}) of MS biochar, but has a markedly influence on the maximum combustion rate (R_{mean}). The R_{max} and R_{mean} values of MS hydrochars prepared at different

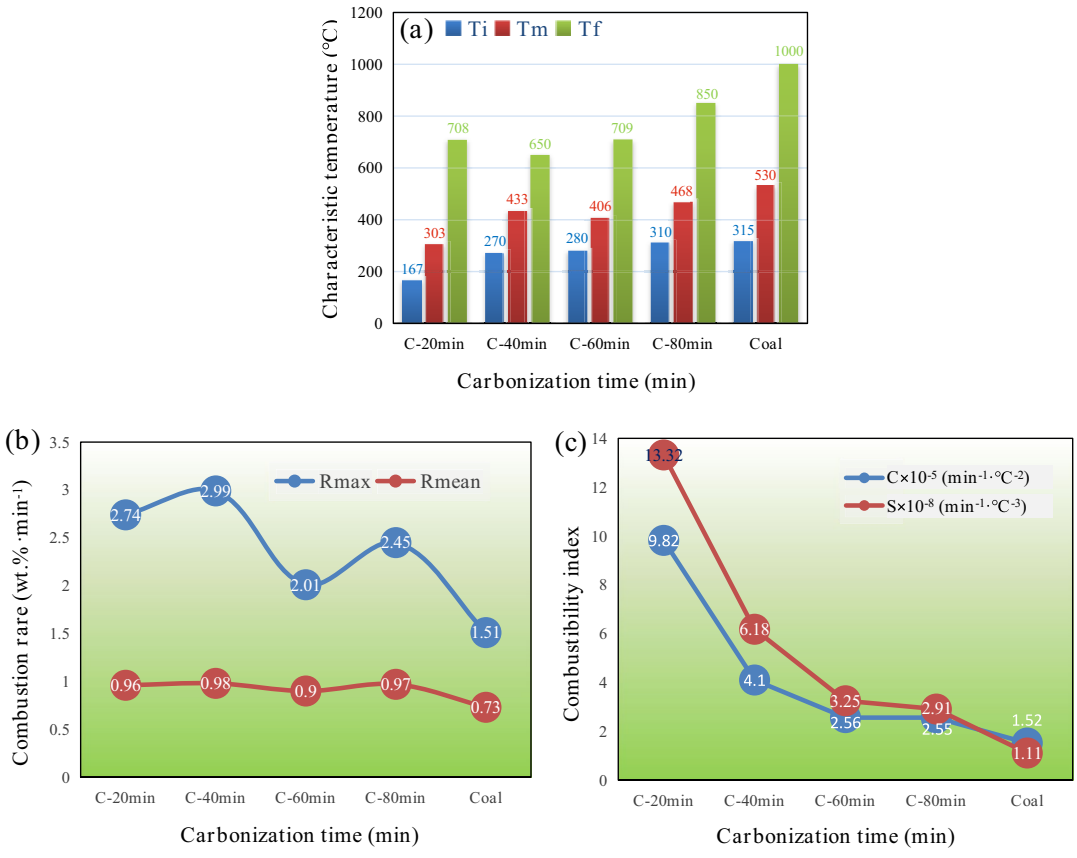

Fig. 14 Effect of carbonization time on the combustion characteristic parameters of MS hydrochars. **a** Characteristic temperature; **b** Combustion rate; **c** Combustibility index

times are significantly larger than that of anthracite, and the highest R_{max} and R_{mean} are observed under the carbonization time is 40 min. It can be seen from Fig. 14c that both the *C* and *S* of MS hydrochars decrease significantly with the increase of carbonization time, indicating that the longer the carbonization time, the higher the carbonization degree and the weaker the combustion reactivity.

Effect of Solid–Liquid Ratio on the Combustion Behavior

The TG and DTG curves of MS hydrochars prepared with various solid–liquid ratios at 260 ℃ for 60 min are shown in Fig. 15, and the corresponding DSC curve is shown in Fig. 16. It can be seen that there is a weak weight loss and endothermic peak before 200 ℃, which is mainly caused by the evaporation of water in the MS hydrochars. When the combustion temperature is 300–850 °C, MS biochar suffers severe combustion loss and heat release. It is worth noting that the solid–liquid ratio has little influence on TG, DTG and DSC curves of MS biochar, which is mainly due to the small difference in chemical composition of MS hydrochars prepared with different solid–liquid ratios.

Figure 17 presents the influence of solid–liquid ratios on the combustion characteristics of MS hydrochars. It can be found that the effect of solid–liquid ratio on characteristic temperature, combustion rate, flammability index and comprehensive combustion characteristic index of carbonized products is not obvious. As shown in Fig. 17a, the T_i, T_m, and T_f of MS hydrochars are 258–272 ℃, 406–448 ℃, and 790–850 ℃, respectively, which are obviously lower than that of anthracite (315 ℃, 530 ℃, and 1000 ℃). As shown in Fig. 17b, the solid–liquid ratio has almost no influence on the Rmax and Rmean of MS biochar. The R_{max} and R_{mean} values of MS hydrochars prepared under different solid–liquid ratios are 2.03–2.37 wt%·min^{-1} and 0.9–0.98 wt%·min^{-1}, respectively. The MS hydrochars present a higher combustion rate than that of anthracite, and the maximum and

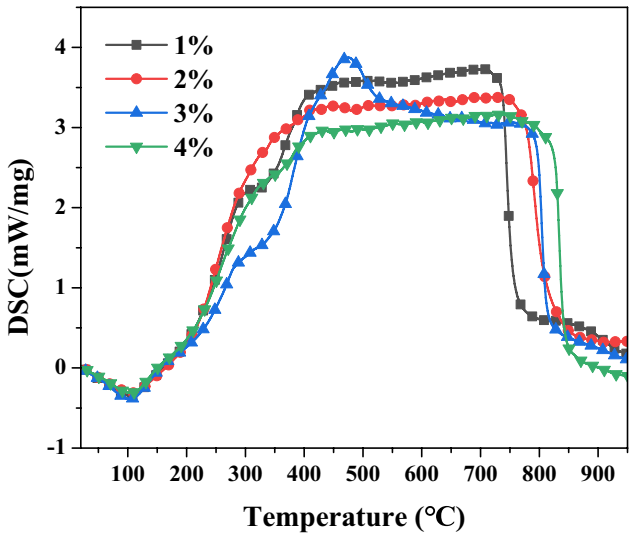

Fig. 16 DSC curves of MS hydrochars prepared at various solid–liquid ratios

average combustion rates of anthracite coal are only 1.51 and 0.73 wt%·min^{-1}, respectively. It can be found from Fig. 17c that the *C* and *S* values of MS hydrochars are obviously higher than that of anthracite. The *C* and *S* values of MS hydrochars prepared at different solid–liquid ratios are 2.78–3.37 and 2.95–3.96, respectively. The *C* and *S* values of anthracite are only 1.52 and 1.11, respectively. This indicates that MS hydrochars have better combustion reactivity than anthracite.

Conclusions

The MS hydrochars were prepared at different hydrothermal carbonization parameters, and the effects of hydrothermal carbonization parameters on physicochemical properties,

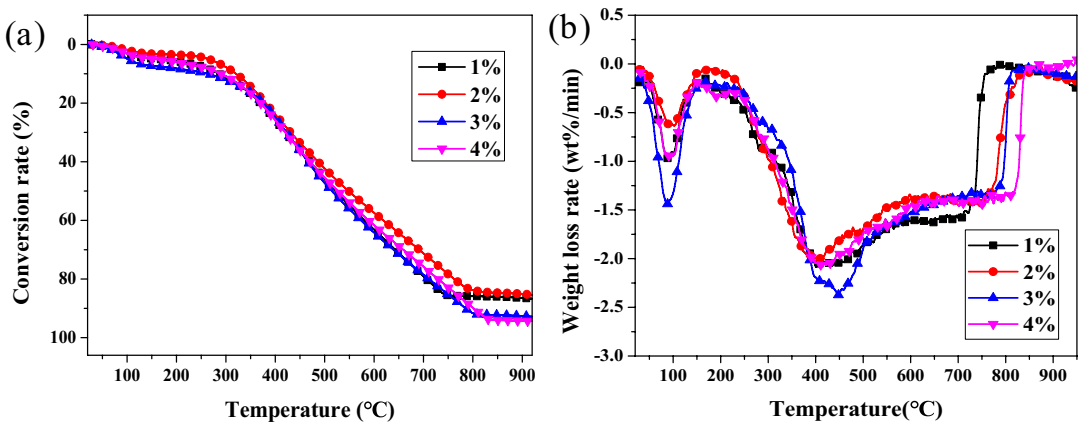

Fig. 15 Combustion conversion rate (**a**) and reaction rate (**b**) curves of MS hydrochars prepared at various solid–liquid ratios

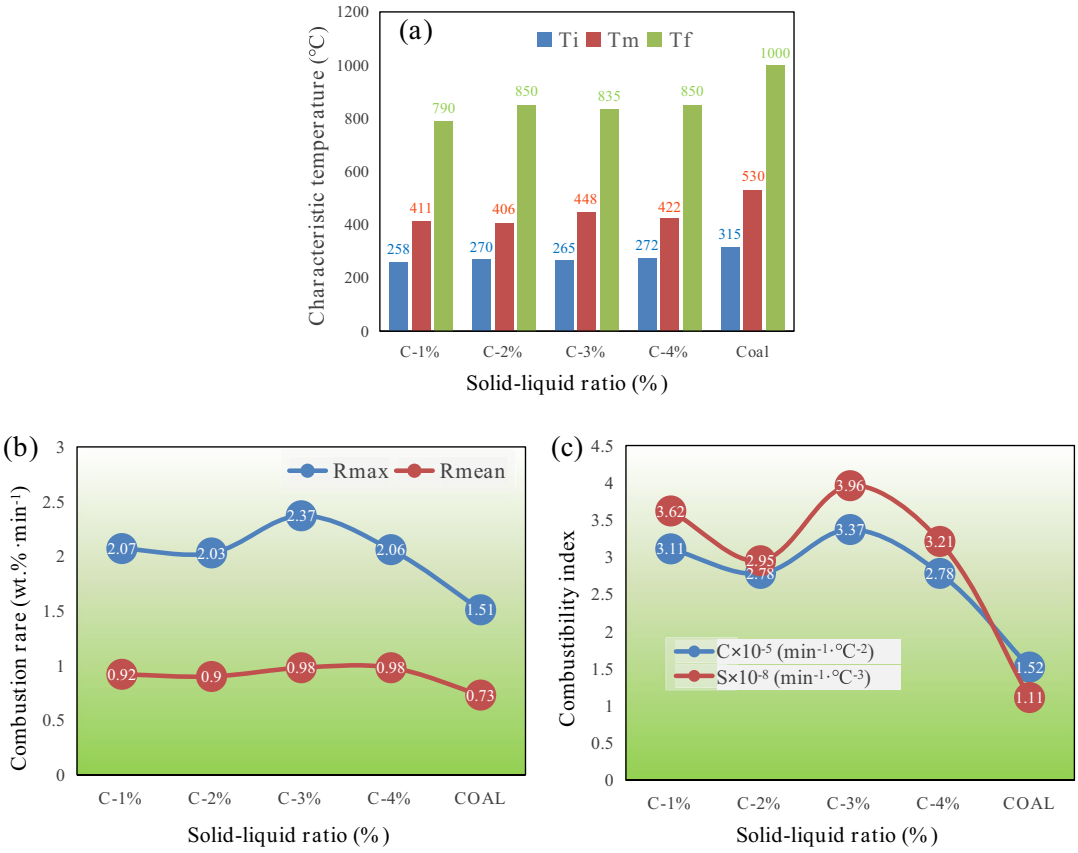

Fig. 17 The effect of solid–liquid ratios on the combustion characteristic parameters of MS hydrochars. **a** Characteristic temperature; **b** Combustion rate; **c** Combustibility index

recovery rate, coalification mechanism and combustion behavior of MS hydrochars were investigated. And the main conclusions are as follows:

(1) The higher the hydrothermal carbonization temperature and the longer the carbonization time, the lower the recovery rate of MS hydrochars. When the carbonization temperature is 260 ℃ and 300 ℃, the recovery rates of MS hydrochars are 20.29% and 14.88%, respectively. Increasing the carbonization temperature and time can effectively improve the dehydration, decarboxylation reaction, and lignin decomposition of MS.

(2) The larger the carbonization temperature and time, the smaller the particle size of the MS hydrochars. On the contrary, with the increase of solid–liquid ratio, the particle size of MS hydrochars increased significantly. Under the optimal carbonization conditions (260℃, 40 min, solid–liquid ratio of 2%), the particle size of MS hydrochar is less than 50 μm, indicating that the MS hydrochar has high reactivity. In addition, the MS hydrochar has a high carbon content and calorific value, and the carbon content and calorific value of MS are 66.85 and 22.36 MJ·kg^{-1}, respectively.

(3) The FC_{ad} content of MS hydrochars significantly increases with the increase of carbonization temperature and time, while the V_{ad} content significantly decreases and the A_{ad} content slightly increases. The influence of solid–liquid ratio on the FC_{ad} and V_{ad} content of carbonization products is relatively small. Increasing the carbonization temperature and solid–liquid ratio will also increase the sulfur content in the MS hydrochars, while increasing the carbonization time will significantly reduce the sulfur content.

(4) The carbonization temperature and time have the greatest effect on the combustion performance of MS hydrochars, while the solid–liquid ratio has a smaller influence. The T_i and T_f of the MS hydrochars show a gradually increasing trend with increasing carbonization temperature and time, while the C and S show a significant downward trend. This indicates that the carbonization degree of MS hydrochars gradually increases, and the combustion reactivity gradually weakens. The MS hydrochars gradually evolve from complex organic compounds to biomass carbon fuels similar to coal powder.

(5) When the carbonization temperature is 260 ℃, the carbonization time is 40 min, and the solid–liquid ratio is 3%, the MS hydrochars have higher yield (32%), fixed carbon content (60.62 wt%), volatile content (22.06 wt%) and lower sulfur content (0.852 wt%). The chemical composition of the carbonization product can meet the requirements of the metallurgical industry.

(6) The T_i and T_m of MS hydrochars are significantly lower than coal powder, while the *C* and *S* are significantly higher than coal powder, indicating that the combustibility and combustion reactivity of MS hydrochars are significantly better than coal powder. The reusable MS hydrochars prepared by hydrothermal carbonization technology has great potential to replace pulverized coal as a metallurgical reducing agent and fuel. The use of zero emission water charcoal can effectively reduce carbon dioxide emissions in the steel industry and have better environmental benefits. However, the density of biomass straw resources is very small, which seriously limits the improvement of hydrothermal carbonization efficiency and the reduction of carbonization cost.

Acknowledgements This work was supported by the Distinguished Youth Research Project of Anhui Provincial Universities (No. 2023AH020019), National Key R&D Program of China (2017YFB0603802) and Open Fund Project of State Key Laboratory of Advanced Steel Process and Materials (RZ2300000011).

Authors Contributions Z.H. Zhang: Investigation, Writing—original draft, Visualization, Formal analysis. X. Shen: Software, Conceptualization, Methodology, Investigation. Yingyi Zhang: Writing—review & editing, Validation, Resources, Supervision, Data curation, Funding acquisition. Zhichen Han: Formal analysis, Investigation, Conceptualization. C.Y. Zhang: Methodology, Investigation.

Data availability Data will be made available on request.

Declarations

Conflict of Interest The authors declare that they have no known competing financial interests or personal relationships that could have appeared to influence the work reported in this paper.

References

1. X.Y. Shi, J. Chang, M. Kim, M.E. Lee, H.Y. Shin, S.O. Han, Isopropanol production using engineered corynebacterium glutamicum from waste rice straw biomass. Bioresour. Technol. (2024). https://doi.org/10.1016/j.biortech.2024.130416
2. Djomdi, H. Fadimatou, B. Hamadou, L.J. Mintsop Nguela, G. Christophe, P. Michaud, Improvement of thermophysical quality of biomass pellets produced from rice husks. Energy Convers. Manage.: X **12**, 100132 (2021). https://doi.org/10.1016/j.ecmx.2021.100132
3. S.F. Dong, Z.Y. Liu, X.Y. Yang, Hydrothermal liquefaction of biomass for jet fuel precursors: a review. Chin. Chem. Lett. (2023). https://doi.org/10.1016/j.cclet.2023.109142
4. M. Heidari, A. Dutta, B. Acharya, S. Mahmud, A review of the current knowledge and challenges of hydrothermal carbonization for biomass conversion. J. Energy Inst. **92**, 1779–1799 (2019). https://doi.org/10.1016/j.joei.2018.12.003
5. S. Yao, Y.J. Zhang, J.X. Xia, T. Xie, Z.B. Zhang, H. Li, J.J. Hu, Cascade utilization of energy in high temperature syngas to reduce energy consumption in biomass gasification processes. Case Stud. Thermal Eng. **52**, 103680 (2023). https://doi.org/10.1016/j.csite.2023.103680
6. J.L. Goldfarb, A.H. Hubble, Q. Ma, M. Volpe, G. Severini, G. Andreottola, L. Fiori, Valorization of cow manure via hydrothermal carbonization for phosphorus recovery and adsorbents for water treatment. J. Environ. Manage. **308**, 114561 (2022). https://doi.org/10.1016/j.jenvman.2022.114561
7. D. Mariuzza, J.C. Lin, M. Volpe, L. Fiori, S. Ceylan, J.L. Goldfarb, Impact of Co-Hydrothermal carbonization of animal and agricultural waste on hydrochars' soil amendment and solid fuel properties. Biomass Bioenerg. **157**, 106329 (2022). https://doi.org/10.1016/j.biombioe.2021.106329
8. L.Y. He, L.J. Duanmu, X.W. Chen, B. You, G. Liu, X. Wen, L. Guo, Q.Y. Bao, J. Fu, W.W. Chen, Regulation of open straw burning and residential coal burning around urbanized areas could achieve urban air quality standards in the cold region of northeastern China. Sustain. Horizons **9**, 100077 (2024). https://doi.org/10.1016/j.horiz.2023.100077
9. Z.W. Wang, W.F. Huang, H. Wang, J. Gao, R.K. Zhang, G.Y. Xu, Z.F. Wang, Research on the improvement of carbon neutrality by utilizing agricultural waste: based on a life cycle assessment of biomass briquette fuel heating system. J. Clean. Prod. **434**, 140365 (2024). https://doi.org/10.1016/j.jclepro.2023.140365
10. S.E. Ibitoye, R.M. Mahamood, T.C. Jen, C. Loha, E.T. Akinlabi, An overview of biomass solid fuels: biomass sources, processing methods, and morphological and microstructural properties. J. Bioresour. Bioprod. **8**, 333–360 (2023). https://doi.org/10.1016/j.jobab.2023.09.005
11. X.G. Liu, S.J. Yuan, X.H. Dai, Thermal hydrolysis prior to hydrothermal carbonization resulted in high quality sludge hydrochar with low nitrogen and sulfur content. Waste Manage. **176**, 117–127 (2024). https://doi.org/10.1016/j.wasman.2024.01.032
12. F.C.P. Ribeiro, J.L. Santos, R.O. Araujo, V.O. Santos, J.S. Chaar, J.A.S. Tenório, L.K.C. de Souza, Sustainable catalysts for esterification: Sulfonated carbon spheres from biomass waste using hydrothermal carbonization. Renew. Energy **220**, 119653 (2024). https://doi.org/10.1016/j.renene.2023.119653
13. Z.H. Zhao, S.L. Qi, R.K. Wang, H.J. Li, G.K. Song, H.J. Li, Q.Q. Yin, Life cycle assessment of food waste energy and resource conversion scheme via the integrated process of anaerobic digestion and hydrothermal carbonization. Int. J. Hydrogen Energy **52**, 122–132 (2024). https://doi.org/10.1016/j.ijhydene.2023.08.203
14. G.Z. Ye, Y.Q. Wang, W.F. Zhu, X.H. Wang, F. Yao, Y.J. Jiao, H.R. Cheng, H.M. Huang, D.Q. Ye, Preparing hierarchical porous carbon with well-developed microporosity using alkali metal-catalyzed hydrothermal carbonization for VOCs adsorption. Chemosphere **298**, 134248 (2022). https://doi.org/10.1016/j.chemosphere.2022.134248
15. L.H. Yu, Y.Y. Zhang, Z.H. Zhang, H.B. Mao, H.S. Han, J.L. Yang, Recycling reuse of municipal sewage sludge in sustainable structural materials: preparation, properties, crystallization and microstructure analyses. Constr. Build. Mater. **398**, 132507 (2023). https://doi.org/10.1016/j.conbuildmat.2023.132507
16. T.A.H. Nguyen, T.H. Bui, W.S. Guo, H.H. Ngo, Valorization of the aqueous phase from hydrothermal carbonization of different feedstocks: challenges and perspectives. Chem. Eng. J. **472**, 144802 (2023). https://doi.org/10.1016/j.cej.2023.144802
17. L.Y. Ma, J.L. Goldfarb, J.D. Song, C. Chang, Q.L. Ma, Enhancing cleaner biomass-coal co-combustion by pretreatment of wheat

straw via washing versus hydrothermal carbonization. J. Clean. Prod. **366**, 132991 (2022). https://doi.org/10.1016/j.jclepro.2022.132991
18. S. Sobek, Q.K. Tran, R. Junga, S. Werle, Hydrothermal carbonization of the waste straw: a study of the biomass transient heating behavior and solid products combustion kinetics. Fuel **314**, 122725 (2022). https://doi.org/10.1016/j.fuel.2021.122725
19. X.W. Xu, R. Tu, Y. Sun, Y.J. Wu, E.C. Jiang, Y.L. Gong, Y. Li, The correlation of physicochemical properties and combustion performance of hydrochar with fixed carbon index. Biores. Technol. **294**, 122053 (2019). https://doi.org/10.1016/j.biortech.2019.122053
20. L. Li, T.T. Han, Y.X. Wu, J.H. Cheng, P.H. Yao, F.Y. Yu, J.J. Zhang, W. Zeng, N.T. Yang, Y.D. Li, Innovative application of tomato straw biochar in direct carbon solid oxide fuel cells for power generation. Catal. Today **430**, 114518 (2024). https://doi.org/10.1016/j.cattod.2024.114518
21. C.Y. Li, Y.X. Feng, F. Zhong, J.M. Deng, T.C. Yu, H.L. Cao, W.J. Niu, Optimization of microwave-assisted hydrothermal carbonization and potassium bicarbonate activation on the structure and electrochemical characteristics of crop straw-derived biochar. J. Energy Storage **55**, 105838 (2022). https://doi.org/10.1016/j.est.2022.105838
22. T.L. Zhang, J.Y. Zhang, S.Z. Wei, Z. Xiong, R.H. Xiao, X. Chuai, Y.C. Zhao, Effect of hydrothermal pretreatment on mercury removal performance of modified biochar prepared from corn straw. Fuel **339**, 126958 (2023). https://doi.org/10.1016/j.fuel.2022.126958
23. J. Böttger, T. Eckhard, C. Pflieger, O. Senneca, M. Muhler, F. Cerciello, Green coal substitutes for boilers through hydrothermal carbonization of biomass: pyrolysis and combustion behavior. Fuel **344**, 128025 (2023). https://doi.org/10.1016/j.fuel.2023.128025
24. P. Yuan, B.X. Shen, D.P. Duan, G. Adwek, X. Mei, F.J. Lu, Study on the formation of direct reduced iron by using biomass as reductants of carbon containing pellets in RHF process. Energy **141**, 472–482 (2017). https://doi.org/10.1016/j.energy.2017.09.058
25. H. Suopajärvi, E. Pongrácz, T. Fabritius, The potential of using biomass-based reducing agents in the blast furnace: a review of thermochemical conversion technologies and assessments related to sustainability. Renew. Sustain. Energy Rev. **25**, 511–528 (2013). https://doi.org/10.1016/j.rser.2013.05.005
26. Y.Y. Zhang, L.H. Yu, K.K. Cui, H. Wang, T. Fu, Carbon capture and storage technology by steel-making slags: recent progress and future challenges. Chem. Eng. J. **455**, 140552 (2023). https://doi.org/10.1016/j.cej.2022.140552
27. Y.Y. Zhang, K.K. Cui, J. Wang, X.F. Wang, J.M. Qie, Q.Y. Xu, Y.H. Qi, Effects of direct reduction process on the microstructure and reduction characteristics of carbon-bearing nickel laterite ore pellets. Powder Technol. **376**, 496–506 (2020). https://doi.org/10.1016/j.powtec.2020.08.059
28. J. Wang, Y.Y. Zhang, K.K. Cui, T. Fu, J.J. Gao, S. Hussain, T.S. AlGarni, Pyrometallurgical recovery of zinc and valuable metals from electric arc furnace dust—a review. J. Clean. Prod. **298**, 126788 (2021). https://doi.org/10.1016/j.jclepro.2021.126788
29. L. Ye, J.L. Zhang, R.S. Xu, X.J. Ning, N. Zhang, C. Wang, X.M. Mao, J.H. Li, G.W. Wang, C. Wang, Co-combustion kinetic analysis of biomass hydrochar and anthracite in blast furnace injection. Fuel **316**, 123299 (2022). https://doi.org/10.1016/j.fuel.2022.123299
30. G.W. Wang, R.G. Li, J.Y. Dan, X. Yuan, J.G. Shao, J.W. Liu, K. Xu, T. Li, X.J. Ning, C. Wang, Preparation of biomass hydrochar and application analysis of blast furnace injection. Energies **16**, 1216 (2023). https://doi.org/10.3390/en16031216
31. H. Suopajärvi, K. Umeki, E. Mousa, A. Hedayati, H. Romar, A. Kemppainen, C. Wang, A. Phounglamcheik, S. Tuomikoski, N. Norberg, A. Andefors, M. Öhman, U. Lassi, T. Fabritius, Use of biomass in integrated steelmaking-Status quo, future needs and comparison to other low-CO_2 steel production technologies. Appl. Energy **213**, 384–407 (2018). https://doi.org/10.1016/j.apenergy.2018.01.060
32. H. Suopajärvi, A. Kemppainen, J. Haapakangas, T. Fabritius, Extensive review of the opportunities to use biomass-based fuels in iron and steelmaking processes. J. Clean. Prod. **148**, 709–734 (2017). https://doi.org/10.1016/j.jclepro.2017.02.029
33. M. Volpe, A. Messineo, M. Mäkelä, M.R. Barr, R. Volpe, C. Corrado, L. Fiori, Reactivity of cellulose during hydrothermal carbonization of lignocellulosic biomass. Fuel Process. Technol. **206**, 106456 (2020). https://doi.org/10.1016/j.fuproc.2020.106456
34. M. Mäkelä, M. Volpe, R. Volpe, L. Fiori, O. Dahla, Spatially resolved spectral determination of polysaccharides in hydrothermally carbonized biomass. Green Chem. **20**(5), 1114–1120 (2018). https://doi.org/10.1039/C7GC03676K